

Zhang, Chen; Celestre, Rafael; Rosenberger, Maik; Notni, Gunther

Exact correction of image distortion in a filter wheel multispectral camera with focus adjustment

Original published in: 2018 Joint IMEKO TC1-TC7-TC13 Symposium: Measurement science challenges in natural and social sciences. - [Bristol] : IOP Publishing, 18 June 2018. - (2018), art. 12031, 6 pp.
ISBN 978-1-5108-6494-8
(Journal of physics. Conference Series ; 1044)

Conference: IMEKO TC1-TC7-TC13 Joint Symposium : (Rio de Janeiro) ; 2017.07.31-08.08

Original published: 2018-06-18

ISSN: 1742-6596

DOI: [10.1088/1742-6596/1044/1/012031](https://doi.org/10.1088/1742-6596/1044/1/012031)

[Visited: 2024-01-25]



This work is licensed under a [Creative Commons Attribution 3.0 Unported license](https://creativecommons.org/licenses/by/3.0/). To view a copy of this license, visit <https://creativecommons.org/licenses/by/3.0/>

Exact correction of image distortion in a filter wheel multispectral camera with focus adjustment

C. Zhang, R. Celestre, M. Rosenberger, G. Notni

Ilmenau University of Technology

Department of Quality Assurance and Industrial Image Processing

Gustav-Kirchhoff-Platz 2, 98693 Ilmenau, Germany

E-mail: chen.zhang@tu-ilmenau.de

Abstract. The correction of inter-channel image distortions in multispectral imaging is the key process for high-precision applications. In this work, image distortion in a special filter wheel camera with sensor actuation based focus adjustment is investigated. Based on the analysis of the optical path, error compensation models at different levels are derived and qualitatively compared with each other. The experimental evaluation of the models shows that the proposed extended radial-tangential model achieves the highest image registration accuracy, especially in the marginal image areas. Furthermore, the stability of these algorithms is evaluated with repeated measurements.

1. Introduction

In multispectral imaging, an accurate registration of the images acquired at different wavelengths is of great advantage to the spatial-spectral analysis of the multispectral image data. A typical multispectral imaging technique is the spectral scanning using a rotating filter wheel with narrow bandpass optical filters. In this technique, the optical aberration originates from the chromatic aberration in the lens, the different spectral refractive indices of the filter materials as well as the deviations in the mechanical filter system, e.g. the different thicknesses and tilt angles of the filters [1] [2]. The optical aberration could be divided into a longitudinal and a transversal part, resulting in an image blurring compared to a reference channel and an image displacement, respectively.

A conventional tool for image sharpness recovery is the image restoration method using point spread function (PSF). In [3] it is shown that a spatially varying free-form PSF model is most suitable for a filter wheel camera system. In [3] a PSF estimation method using a random noise target is proposed to calculate the relative PSFs relating to the reference channel, and in [4] the blind restoration method is adapted for the PSF characterization. Due to the block-wise PSF estimation used in these works the channel images must be geometrically aligned with each other before the PSF estimation. With a large spectral range, the blurring due to longitudinal aberration could be extremely significant and disturbs this geometric image alignment. Moreover, the performance of image restoration method is strongly limited with heavy blurring, and irregular distortions could be produced due to the anisotropic free-form PSF model. Therefore, mechanical focus correction methods could be more meaningful for high-precision measurements.

In a previous work of the authors [5], a focus adjustment via mounting glass correction plates at the filters is implemented. On this basis, a 2D polynomial function is estimated for the correction of image displacements. With this method, about 95% of the image distortion could be removed. However, this



focus correction approach counts only for the special objective as well as working distance. In order to facilitate a higher flexibility concerning the change of objective and variation of working distance, an autofocus approach via linear sensor actuation is developed in a following work [6]. Nevertheless, the sensor actuation in this approach causes a variation of the distance between the objective and image sensor, leading to an alteration of the imaging characteristics. In this work, the image distortion in this circumstance and its compensation will be analyzed and experimentally investigated.

2. Theoretical analysis of the transversal aberration

In the focus correction, the channel of 550 nm is set as reference channel due to its high signal-to-noise ratio. In this channel, a perfect focusing is realized with manual lens adjustment. Afterwards, the sensor positions for the best focusing in the other channels are estimated through maximization of the graph Laplacian energy at a target object. In this work, the image distortion is defined as the relative image displacement in comparison to the reference channel and includes all the influences of filter aberration, lens chromatic aberration, lens distortion, sensor actuation as well as all the machining and mounting deviations in the mechanical guide.

2.1. Filter aberration under linear sensor actuation

In a previous work of the authors [7], the optical aberration caused by the filters with regard to the variation of the sensor-aperture-distance (focal length) is analysed. The relative filter aberration in comparison to the reference channel is dependent on the refractive indices of both filter materials n and n_{ref} , the filter normal vectors \mathbf{n} and \mathbf{n}_{ref} , the sensor positions d_s and $d_{s,ref}$ as well as a transversal shift of the sensor \mathbf{S}_s concerning the positioning errors of the mechanical guide. It is proved that the image point displacement $\mathbf{e}_{F,rel}$ caused by the filter aberration and sensor actuation consists of a global part and a location dependent part, which could be modelled as a shift of the image principle point and an image zoom, respectively, under the paraxial approximation.

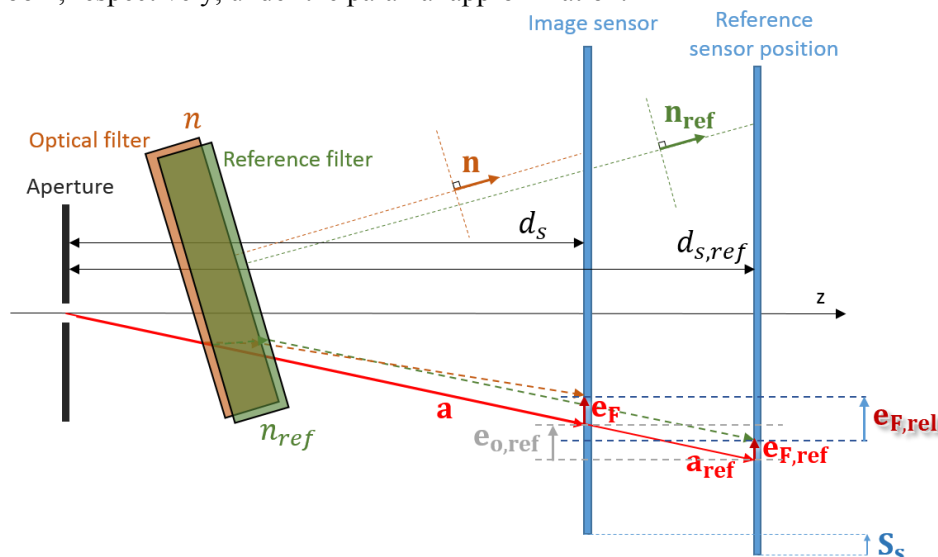


Figure 1: Filter aberration under linear sensor actuation.

2.2. Lens chromatic aberration and lens distortion

Under a perfect focus correction and the paraxial approximation, it is obvious that the linear sensor actuation for the compensation of the longitudinal aberration leads to a lateral image displacement $\mathbf{e}_{c,rel}$ in figure 2 that corresponds to the shift $\mathbf{e}_{o,rel}$ in figure 1. It indicates that an explicit modelling of the transversal lens chromatic aberration is not needed in this ideal case. Considering the risk of an imperfect focus correction or a large field of view that could disturb the paraxial approximation, the

affine model [2] and radial-tangential model in [8] proposed for filter wheel cameras with fixed sensor position will be taken as reference models.

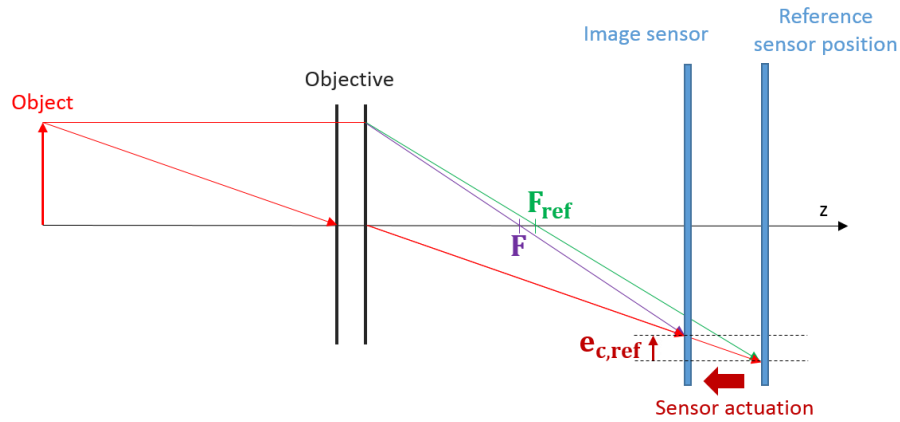


Figure 2: Transversal chromatic aberration in sensor actuation.

Next to the lens chromatic aberration, the channel dependence of the lens distortion could also take a considerable part in the total image distortion. The lens distortion is influenced by the wavelength-dependent refractive index of lens material [9] as well as the image sensor position. Furthermore, the shift of the image principle point, which is usually assumed as the distortion-free reference point, causes also an alteration of the lens distortion parameters relating to the local image coordinate system and could be several pixels due to the mechanics [6]. The channel dependence of lens distortion could be more remarkable in the image areas with severe distortions, mostly the marginal areas. For the requirement for a higher precision, the channel dependence of lens distortion could be also taken into consideration by the means of a channel-wise correction.

3. Proposed image correction models

3.1. Scaling-translation model

According to the analysis in section 2, image correction models at different levels can be derived. Assuming a perfect focus adjustment and ignoring the channel dependence of lens distortion, a simple scaling-translation model (ST model) can be used with parameters k_1 to k_3 :

$$\begin{pmatrix} x_d \\ y_d \end{pmatrix} = \begin{pmatrix} k_1 x_n + k_2 \\ k_1 y_n + k_3 \end{pmatrix}, \quad (1)$$

where (x_d, y_d) and (x_n, y_n) denote the locations of distorted and undistorted image point referring to the image principle point that is simultaneously estimated in the model fitting.

3.2. Affine model

As a reference model, the combination of the ST model with the affine model for chromatic aberration in [2] could be used. An affine transformation consists of a rotation, a translation and an anisotropic scaling, and allows a finer modelling of the possible irregularity of distortions. Because that it contains already the ST model, this combination results in an affine image correction model in turn.

3.3. Channel-wise lens distortion correction

In order to deal with the channel dependence of lens distortion, a channel-wise correction is performed before the implementation of these both aforementioned models. For the correction, the lens distortion model in [10] is used:

$$\begin{pmatrix} x_d \\ y_d \end{pmatrix} = \begin{pmatrix} x_n(1 + d_1 r^2 + d_2 r^4) + 2d_3 x_n y_n + d_4(r^2 + 2x_n^2) \\ y_n(1 + d_1 r^2 + d_2 r^4) + d_3(r^2 + 2y_n^2) + 2d_4 x_n y_n \end{pmatrix}, \quad (2)$$

where r denotes the distance between the undistorted image point and the principle point, and d_i are the lens distortion coefficients.

3.4. Radial-tangential model

Under the fact that the polynomial terms in the radial-tangential chromatic aberration model in [8] are already contained in the lens distortion model in [10], an extended radial-tangential model (RT model) combing the filter aberration, lens chromatic aberration and lens distortion is proposed as follows:

$$\begin{pmatrix} x_d \\ y_d \end{pmatrix} = \begin{pmatrix} x_n(1+k_1+k_2r^2+k_3r^4)+2k_4x_ny_n+k_5(r^2+2x_n^2)+k_6 \\ y_n(1+k_1+k_2r^2+k_3r^4)+k_4(r^2+2y_n^2)+2k_5x_ny_n+k_7 \end{pmatrix}, \quad (3)$$

where k_i are the model parameters.

Due to the large number of model parameters, the implementation of the RT model succeeds in three steps. In the first step, the image translation and zoom parameters as well as the image principle point are estimated using the least squares method. Then, these parameters are fixed, and the parameters in the radial and tangential terms of higher degree are estimated. In the last step, all the model parameters are refined again through the Levenberg-Marquardt optimization.

4. Experimental results

Experimental investigations are performed at a 12-channel filter wheel camera. The spectral channels are between 400 nm and 950 nm in step of 50 nm and have a full width at half maximum (FWHM) of 50 nm. As target object, a dot grid glass target is placed orthogonal to the camera in a distance of ca. 400 mm and illuminated with uniform backlight. For the acquisition, the objective Carl Zeiss Tevidon 1.4/25 is used. In order to exclude the influences of vibration caused by the sensor actuation, a latency of 0.5 seconds between channel switch and image acquisition is specified.

For the extraction of the circular markers on the target, the two-step procedure in [11] is used. The markers are roughly detected based on Hough transform, and the centers of the dots are then located with higher accuracy using the search-line based edge point detection and circle fitting. These centers are used as controlling points for the model evaluation. Deviations between the dot centers detected in the corrected channel images and the reference image are identified as residual errors.

4.1. Model evaluation

In order to oppress stochastic errors, the model parameter estimation is performed with ten repeated full spectral acquisitions, whereby the dots are repetitively detected and their coordinates are averaged. From the raw image data, the mean and maximal errors in each channel are determined and averaged across all the channels. The cross-channel mean error is 2.958 pixels, and the maximal error among the channels is 8.326 pixels with an averaged maximal error of 4.67 pixels.

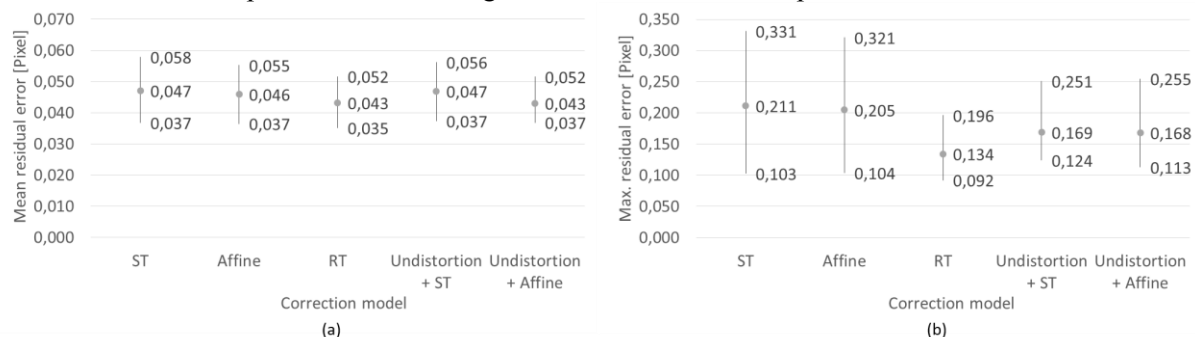


Figure 3: Model evaluation results: cross-channel mean (a) and maximal residuals (b).

Figure 3 shows the cross-channel mean and maximal residual errors in the corrected image data, with an indication of the maximal and minimal values among the channels. It can be seen that the cross-channel mean residual could be reduced to lower than 0.05 pixels with all the models. Among these

models, the RT model exhibits a minor advantage at thousandth pixel level. This is yet negligible in practical applications.

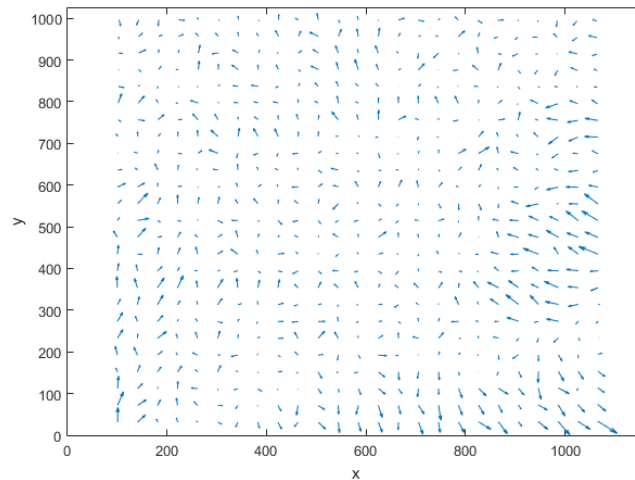


Figure 4. Residual errors with the extended RT model in 900 nm channel.

In comparison to the mean residual error, the maximum residual is much larger. As an example, the residual errors in the 900 nm channel at the RT model are presented in figure 4, in which the residual errors are drawn as vectors at the controlling points. It could be seen that the residuals in the marginal areas of the image are more significant, which correspond to areas with stronger lens distortion. By the means of explicit lens distortion correction, the cross-channel maximal residual error can be reduced from ca. 0.21 pixels to ca. 0.17 pixels at the ST and affine model. A more considerable advantage of the RT model is recognizable. With this model, a cross-channel maximal residual of 0.134 pixels is achieved, while the upper limit is lower than with other models.

4.2. Performance evaluation with repeated measurements

As a next step, the stability of the image correction methods is evaluated with repeated measurements. This evaluation is performed with ten further spectral acquisitions that are corrected using the model parameters estimated in section 4.1. At each spectral acquisition the cross-channel averaged mean and maximal residual are determined. Table 1 shows that the models exhibit almost the same performance relating to the cross-channel mean residual, with a minor general growth than the values in section 4.1.

Table 1. Mean and standard deviation of cross-channel mean residual.

	ST	Affine	RT	Undistortion + ST	Undistortion + Affine
Mean	0.063	0.061	0.060	0.063	0.059
Standard deviation	0.003	0.003	0.002	0.002	0.002

Table 2. Mean and standard deviation of cross-channel maximal residual.

	ST	Affine	RT	Undistortion + ST	Undistortion + Affine
Mean	0.225	0.211	0.173	0.190	0.183
Standard deviation	0.022	0.022	0.009	0.013	0.009

The evaluation concerning the cross-channel maximal residual reflects also the same trend in section 4.1, see table 2. Overall, a cross-channel mean residual of 0.060 ± 0.002 pixels and maximal residual of 0.173 ± 0.009 pixels are achieved with the extended RT model. These lower values could validate the advantages of the RT model over the other models, primarily in the marginal image areas.

5. Conclusion and future work

The experimental results show that the simple scaling-translation (ST) model can already compensate more than 98% of image distortion. It indicates the correctness of the theoretical analysis and a high-precision focus correction. The affine model remains nearly at the same level as the ST model, while these both models suffer from the irregular lens distortion in the marginal image areas. An explicit correction of lens distortion scores an improvement, but could produce additional process errors and is hence less accurate than the extended radial-tangential (RT) model. With a higher comprehensiveness, the RT model ensures a more accurate compensation of image distortion in the marginal image areas and hence a mitigation of artefacts in multispectral image processing that could be caused by inter-channel pixel displacements. So, the RT model could be implemented for high-precision geometric and color measurements as well as spatio-spectral analysis, in which the entire area of the image sensor should be used.

The measurement uncertainty with this filter wheel camera arises from the illumination fluctuation and mechanical sensor actuation, whereas the last one concerning the accuracy and uncertainty of sensor repositioning could play a crucial role. In high-speed acquisitions, a higher sensor actuation frequency could cause a stronger vibration and lead to an increased measurement uncertainty. Evaluation of the error compensation algorithms in this case will be performed as a future work.

Acknowledgements

We thank the Federal Ministry of Education and Research for the strong support of this work. The work is related to the project *Qualimess next generation* (03IPT709X) and the program *Zwanzig20 – Partnership for Innovation* as part of the research alliance 3Dsensation.

References

- [1] Brauers J and Aach T 2008 Longitudinal Aberrations Caused by Optical Filters and Their Compensation in Multispectral Imaging *Proc. of 2008 IEEE International Conference on Image Processing (ICIP2008)* 525-528
- [2] Brauers J, Schulte N and Aach T 2008 Multispectral Filter-Wheel Cameras: Geometric Distortion Model and Compensation Algorithms *IEEE Transactions on Image Processing* **17** 2368-2380
- [3] Brauers J, Seiler C and Aach T 2010 Direct PSF Estimation Using a Random Noise Target *Proc. SPIE 7537, Digital Photography VI*, 75370B
- [4] Klein J 2015 *Multispectral imaging: aberrations and acquisitions from different viewing positions* (RWTH Aachen University, PhD thesis)
- [5] Rosenberger M and Linss G 2015 Multispectral Image Correction for Geometric Measurement *Journal of Physics: Conference Series* **588** 012037
- [6] Rosenberger M, Preissler M, Fuetterer R, Zhang C, Celestre R and Notni G 2016 Development and characterization of a high speed linear-moving-stage for multispectral measurements *Journal of Physics: Conference Series* **772** 012054
- [7] Zhang C, Rosenberger M, Breitbarth A and Notni G 2016 A novel 3D multispectral vision system based on filter wheel cameras *Proc. of 2016 IEEE International Conference on Imaging Systems and Techniques (IST 2016)* 267-272
- [8] Klein J, Brauers J and Aach T 2010 Spatial and Spectral Analysis and Modeling of Transversal Chromatic Aberrations and their Compensation *Proc. of IS&Ts 5th European Conference on Color in Graphics, Imaging, and Vision (CGIV)* 516-522
- [9] Haferkorn H 1986 *Bewertung optischer Systeme* (Berlin: Deutscher Verlag der Wissenschaften)
- [10] Brauer-Burchardt C 2005 A new methodology for determination and correction of lens distortion in 3D measuring systems using fringe projection *Pattern Recognition* **3663** 200-207
- [11] Breitbarth A, Correns M, Zimmermann Z, Zhang C, Rosenberger M, Schambach J and Notni G 2017 Verification of real sensor motion for a high-dynamic 3D measurement inspection system *Proc. SPIE 10329, Optical Measurement Systems for Industrial Inspection X*, 10329-22